IMPROVED PARTICLE FILTERS FOR BALLISTIC TARGET TRACKING

Marcelo G. S. Bruno and Anton Pavlov

Instituto Tecnológico de Aeronáutica
São José dos Campos SP 12228-900, Brazil
ph:(55-12) 3947-5878; email: {bruno,anton}@ele.ita.br

ABSTRACT

We present in this paper two improved particle filter algorithms for ballistic target tracking. The first algorithm is a sampling/importance resampling (SIR) filter that uses an optimized importance function plus residual resampling to combat particle degeneracy, and also incorporates a Metropolis-Hastings (MH) move step to reduce particle impoverishment. The second proposed algorithm is an auxiliary particle filter (APF). Both algorithms show good performance results when compared to the ideal posterior Cramér-Rao lower bound for the mean square estimation error.

1. INTRODUCTION

We propose in this paper improved particle filter algorithms for automatic tracking of supersonic ballistic targets in the phase of reentry into the atmosphere. The goal is to estimate in a recursive fashion the unknown kinematic state, e.g. position and velocity, of the target given a sequence of noisy position measurements generated by a conventional radar. In general, a closed-form analytical expression for the minimum mean square error (MMSE) estimate of the hidden state cannot be obtained in the ballistic target tracking problem due to nonlinearities both in the state dynamic model and in the observation (measurement) model. We resort then to a sequential importance sampling method, referred to in the literature as particle filtering [1], to approximate the optimal MMSE estimate.

Farina et al. proposed in [2] the application of a bootstrap particle filter [3] to the problem of ballistic target tracking assuming a nonlinear target motion model and a linear observation model, with both models specified in cartesian coordinates. In this paper, we use the same motion model as in [2], but assume an alternative nonlinear observation model in polar coordinates. Furthermore, instead of using the standard bootstrap filter, we design a different sampling/importance resampling (SIR) tracker where we apply the local linearization technique in [4] to optimize the choice of the importance sampling function. We also use this locally optimized importance sampling function to design an additional Markov Chain Monte Carlo (MCMC) move step, see e.g. [5], which is introduced after the resampling step to minimize particle impoverishment. As an alternative to the optimized SIR filter described before, we also present in the paper an auxiliary particle filter (APF) tracker based on the technique introduced in [6]. The root mean-square error (RMSE) curves for the optimized SIR filter and the APF are obtained through Monte Carlo simulations and compared to the square root of the posterior Cramér-Rao lower bound (CRLB), which is estimated from the same set of simulated data using the algorithm proposed in [7].

This paper is divided into 5 sections. Section 1 is this Introduction. In Section 2, we review briefly the target motion and the radar measurement models. In Section 3, we present the proposed particle filter trackers. In Section 4, we discuss the performance of our algorithms . Finally, Section 5 summarizes the main results in the paper.

2. THE MODEL

Let k be a non-negative integer number and denote by Δ the time interval between two consecutive radar measurements. Assuming for simplicity a flat Earth, define the unknown target state vector at instant $t = k\Delta$ as the four-dimensional vector $\mathbf{s}_k = [x_k\ \dot{x}_k\ y_k\ \dot{y}_k]^T$, that collects the positions, x_k and y_k, and the velocities, $\dot{x}_k$ and $\dot{y}_k$, of the target in a system of 2D cartesian coordinates (x, y). We describe the motion of a ballistic target in the phase of reentry into the atmosphere by the discrete-time nonlinear dynamic system [2]

$$\mathbf{s}_{k+1} = \mathbf{\Phi}\mathbf{s}_k + \mathbf{G}\mathbf{f}(\mathbf{s}_k) + \mathbf{G}\begin{bmatrix}0\\-g\end{bmatrix} + \mathbf{w}_k \qquad (1)$$

where g is the gravity acceleration (assumed constant), matrices $\mathbf{\Phi}$ and $\mathbf{G}$ are given by

$$\mathbf{\Phi} = \begin{bmatrix}1 & \Delta & 0 & 0\\0 & 1 & 0 & 0\\0 & 0 & 1 & \Delta\\0 & 0 & 0 & 1\end{bmatrix}, \quad \mathbf{G} = \begin{bmatrix}\frac{\Delta^2}{2} & 0\\\Delta & 0\\0 & \frac{\Delta^2}{2}\\0 & \Delta\end{bmatrix} \qquad (2)$$

The work of the second author was supported by CAPES, Brazil.

and $\{\mathbf{w}_k\}$, $k \geq 0$ is a sequence of independent, identically distributed (i.i.d.) Gaussian random vectors, with zero mean and non-singular covariance matrix

$$\mathbf{Q} = q \begin{bmatrix} \mathbf{\Theta} & \underline{0} \\ \underline{0} & \mathbf{\Theta} \end{bmatrix}, \qquad \mathbf{\Theta} = \begin{bmatrix} \frac{\Delta^3}{3} & \frac{\Delta^2}{2} \\ \frac{\Delta^2}{2} & \Delta \end{bmatrix} \tag{3}$$

where q is a positive real number. Finally, the nonlinear function $\mathbf{f}$ in (1) corresponds to the drag force that is computed by the expression [2]

$$\mathbf{f}(\mathbf{s}_k) = -0.5 \frac{g}{\beta} \rho(s_k[3]) \sqrt{s_k^2[2] + s_k^2[4]} \begin{bmatrix} s_k[2] \\ s_k[4] \end{bmatrix}. \tag{4}$$

In (4), the parameter β denotes the target ballistic coefficient, also assumed constant. The parameter ρ represents the air density which decays according to the exponential law $\rho(y) = c_1 \exp(-c_2 y)$ where $c_1 = 1.227$, $c_2 = 1.093 \times 10^{-4}$ for $y < 9144\ m$, and $c_1 = 1.754$, $c_2 = 1.49 \times 10^{-4}$ for $y \geq 9144\ m$.

2.1. Observation Model

A conventional tracking radar generates at each instant k noisy measurements $\mathbf{z}_k = [z_{1,k}\ z_{2,k}]^T$ respectively of the range and elevation of the target. The radar measurements are related to the hidden state $\mathbf{s}_k$ by the nonlinear observation model

$$\mathbf{z}_k = \underbrace{\begin{bmatrix} \sqrt{s_k^2[1] + s_k^2[3]} \\ \arctan(\frac{s_k[3]}{s_k[1]}) \end{bmatrix}}_{\mathbf{h}(\mathbf{s}_k)} + \underbrace{\begin{bmatrix} v_{r,k} \\ v_{\epsilon,k} \end{bmatrix}}_{\mathbf{v}_k} \tag{5}$$

where $\{v_{r,k}\}$ and $\{v_{\epsilon,k}\}$ are two mutually independent, Gaussian i.i.d. random sequences with zero mean and variances respectively σ_r^2 and σ_ϵ^2 such that the covariance matrix $\mathbf{R} = E\left[\mathbf{v}_k\, \mathbf{v}_k^T\right]$ is diagonal with $R(1,1) = \sigma_r^2$ and $R(2,2) = \sigma_\epsilon^2$, for any $k \geq 0$. In (5), we assumed that the true target elevation angle lies between 0 and $\pi/2$. Otherwise, it suffices to add π to the $\arctan$ term in (5).

3. PARTICLE FILTER TRACKING ALGORITHMS

Let $\mathbf{Z}_1^k = \{\mathbf{z}_1, \mathbf{z}_2, \ldots, \mathbf{z}_k\}$ be a sequence of observations. Particle filtering, see [1], is a sequential importance sampling method that recursively generates a properly weighted set of samples (or particles) $\left\{\mathbf{s}_k^{(j)}\right\}$, with associated weights $w_k^{(j)}$, $j = 1, 2, \ldots, N_p$, such that, as $N_p \to \infty$, the weighted average of the particles at each instant k converges (in some statistical sense) to the optimal MMSE estimate $E\left[\mathbf{s}_k \mid \mathbf{Z}_1^k\right]$ of the hidden state. The initial particle set is sampled $\mathbf{s}_0^{(j)} \sim p(\mathbf{s}_0)$ with weights $w_0^{(j)} = 1/N_p$, $j = 1, \ldots, N_p$. The subsequent particle populations $\left\{\mathbf{s}_k^{(j)}\right\}$, $k > 0$, are generated by sequentially sampling from a given importance probability density function, and the corresponding weights are recursively updated, see [1], using the state dynamic model, the observation model, and the chosen importance function.

3.1. Improved SIR Particle Filter

The main drawback associated with sequential importance sampling is that the variance of the importance weights increases with time, leading to particle degeneracy [1]. One way to mitigate particle degeneracy is to draw the jth particle at instant k from the optimal importance function $p(\mathbf{s}_k \mid \mathbf{s}_{k-1}^{(j)}, \mathbf{z}_k)$, see [4], that minimizes the variance of the importance weights conditioned on the simulated particle trajectories and on the observations.

Optimal Importance Function Approximation Assuming that $\{\mathbf{v}_k\}$, $\{\mathbf{w}_k\}$ and $\mathbf{s}_0$ are mutually independent, it follows from Bayes' law and the Markovian model assumption that

$$p(\mathbf{s}_k \mid \mathbf{s}_{k-1}^{(j)}, \mathbf{z}_k) = \frac{p(\mathbf{z}_k \mid \mathbf{s}_k)\, p(\mathbf{s}_k \mid \mathbf{s}_{k-1}^{(j)})}{p(\mathbf{z}_k \mid \mathbf{s}_{k-1}^{(j)})} \tag{6}$$

To approximate the optimal importance function in (6), we resort to the local linearization technique described in [4]. Define first $\mathbf{\Psi}(\mathbf{s}_k)$ as the function

$$\mathbf{\Psi}(\mathbf{s}_k) = \mathbf{\Phi}\mathbf{s}_k + \mathbf{G}\mathbf{f}(\mathbf{s}_k) + \mathbf{G}\begin{bmatrix} 0 \\ -g \end{bmatrix} \tag{7}$$

where $\mathbf{\Phi}$, $\mathbf{G}$, and $\mathbf{f}(.)$ are defined as in (2) and (4). Expanding now the observation equation (5) around $\mathbf{\Psi}(\mathbf{s}_{k-1}^{(j)})$, we make the first-order approximation

$$\mathbf{z}_k \approx \mathbf{h}\left[\mathbf{\Psi}(\mathbf{s}_{k-1}^{(j)})\right] + \mathbf{H}_k^{(j)}\left[\mathbf{s}_k - \mathbf{\Psi}(\mathbf{s}_{k-1}^{(j)})\right] + \mathbf{v}_k \tag{8}$$

where $\mathbf{H}_k^{(j)} = \nabla\mathbf{h}(\mathbf{s})$ evaluated at $\mathbf{s} = \mathbf{\Psi}(\mathbf{s}_{k-1}^{(j)})$, and the nonlinear function $\mathbf{h}(.)$ is defined in (5). For equation (5),

$$\nabla\mathbf{h}(\mathbf{s}) = \begin{bmatrix} \frac{s[1]}{\sqrt{s^2[1]+s^2[3]}} & 0 & \frac{s[3]}{\sqrt{s^2[1]+s^2[3]}} & 0 \\ \frac{-s[3]}{s^2[1]+s^2[3]} & 0 & \frac{s[1]}{s^2[1]+s^2[3]} & 0 \end{bmatrix}. \tag{9}$$

Let now $N(\mathbf{s} - \mathbf{a}, \mathbf{P})$ denote the multivariable normal function of argument $\mathbf{s}$, mean $\mathbf{a}$ and covariance matrix $\mathbf{P}$. It can be shown after a simple algebraic exercise that, for the nonlinear state model in (1) and the linearized observation model in (8), equation (6) reduces to

$$p(\mathbf{s}_k \mid \mathbf{s}_{k-1}^{(j)}, \mathbf{z}_k) = N(\mathbf{s}_k - \mathbf{m}_k^{(j)},\, \mathbf{\Sigma}_k^{(j)}) \tag{10}$$

where

$$\mathbf{\Sigma}_k^{(j)} = \left[\mathbf{Q}^{-1} + (\mathbf{H}_k^{(j)})^T \mathbf{R}^{-1} (\mathbf{H}_k^{(j)})\right]^{-1} \tag{11}$$

$$\begin{aligned} \mathbf{m}_k^{(j)} &= (\Sigma_k^{(j)}) \Big\{ \mathbf{Q}^{-1}\mathbf{\Psi}(\mathbf{s}_{k-1}^{(j)}) + (\mathbf{H}_k^{(j)})^T \mathbf{R}^{-1} \\ &\times \left[\mathbf{z}_k - \mathbf{h}(\mathbf{\Psi}(\mathbf{s}_{k-1}^{(j)}) + \mathbf{H}_k^{(j)}\mathbf{\Psi}(\mathbf{s}_{k-1}^{(j)})\right] \Big\} \end{aligned} \tag{12}$$

Importance Weights Update After sampling the jth particle $\tilde{\mathbf{s}}_k^{(j)} \sim p(\mathbf{s}_k \mid \mathbf{s}_{k-1}^{(j)}, \mathbf{z}_k)$, the corresponding importance weight $\tilde{w}_k^{(j)}$ is updated using the recursion

$$\tilde{w}_k^{(j)} \infty w_{k-1}^{(j)} \frac{N(\mathbf{z}_k - \mathbf{h}(\mathbf{s}_k^{(j)}), \mathbf{R})\, N(\mathbf{s}_k^{(j)} - \mathbf{\Psi}(\mathbf{s}_{k-1}^{(j)}), \mathbf{Q})}{N(\mathbf{s}_k^{(j)} - \mathbf{m}_k^{(j)},\, \mathbf{\Sigma}_k^{(j)})} \tag{13}$$

where the symbol ∞ denotes "proportional to". The proportionality constant is computed such that $\sum_j \tilde{w}_k^{(j)} = 1$.
Selection Step We can further reduce particle degeneracy by adding a selection step [3] that consists of resampling a new particle set $\left\{\overline{\mathbf{s}}_k^{(j)}\right\}$ from the original set $\left\{\tilde{\mathbf{s}}_k^{(j)}\right\}$ with replacement according to the weights $\tilde{w}_k^{(j)}$. After the resampling, all particle weights are then reset to $\overline{w}_k^{(j)} = 1/N_p$, $j = 1, \ldots, N_p$. To speed up computations, we use the *residual resampling* method [8] only when the approximate effective number of particles $N_{eff} = \left[\sum_j (\tilde{w}_k^{(j)})^2\right]^{-1}$, see [1], falls below 60 % of the total number of particles.

MCMC Move Step In order to restore particle diversity after the resampling step, we follow the lead in [5] and add a Metropolis-Hastings (MH) move step that moves the weighted particle set $\left\{\overline{\mathbf{s}}_k^{(j)}, 1/N_p\right\}$ to a new weighted sample set $\left\{\mathbf{s}_k^{(j)}, 1/N_p\right\}$ using the importance function $N(\mathbf{s}_k - \mathbf{m}_k^{(j)}, \mathbf{\Sigma}_k^{(j)})$ as proposal density. Specifically, let

$$w^*(\mathbf{s}_k^{(j)}) = \frac{N(\mathbf{z}_k - \mathbf{h}(\mathbf{s}_k^{(j)}), \mathbf{R})\, N(\mathbf{s}_k^{(j)} - \mathbf{\Psi}(\mathbf{s}_{k-1}^{(j)}), \mathbf{Q})}{N(\mathbf{s}_k^{(j)} - \mathbf{m}_k^{(j)},\, \mathbf{\Sigma}_k^{(j)})}\,. \tag{14}$$

The proposed MH move step for $j = 1, \ldots, N_p$ is
- Sample $\widehat{\mathbf{s}}_k^{(j)} \sim N(\mathbf{s}_k - \mathbf{m}_k^{(j)}, \mathbf{\Sigma}_k^{(j)})$.
- Sample $u \sim \mathcal{U}([0,1])$ and make the decision

$$\begin{array}{lll} \text{If } u \le \min\left\{1, \frac{w^*(\widehat{\mathbf{s}}_k^{(j)})}{w^*(\overline{\mathbf{s}}_k^{(j)})}\right\} & \mathbf{s}_k^{(j)} = \widehat{\mathbf{s}}_k^{(j)} & \text{(accept move)} \\ \text{else} & \mathbf{s}_k^{(j)} = \overline{\mathbf{s}}_k^{(j)} & \text{(reject move).} \end{array}$$

3.2. Auxiliary Particle Filter

A possible alternative to the improved SIR filter presented in subsection 3.1 is to use auxiliary particle filtering [6]. We choose $p(\mathbf{s}_k \mid \mathbf{s}_{k-1}^{(j)})$ as importance function, but use an auxiliary index variable to pre-select particles at instant $k-1$ that, when propagated to the next time step, are more likely to have a high likelihood. The modified importance sampling algorithm for $j = 1, \ldots, N_p$ becomes
- Sample $\underline{\mu}_k^{(j)} \sim N(\mathbf{s}_k - \mathbf{\Psi}(\mathbf{s}_{k-1}^{(j)}), \mathbf{Q})$.
- Compute $\lambda_k^{(j)} \infty w_{k-1}^{(j)} N(\mathbf{z}_k - \mathbf{h}(\underline{\mu}_k^{(j)}), \mathbf{R})$.
- Sample $i^{(j)} \sim \{1, \ldots, N_p\}$ with $P(\{i^{(j)} = l\}) = \lambda_k^{(l)}$.
- Sample $\mathbf{s}_k^{(j)} \sim N(\mathbf{s}_k - \mathbf{\Psi}(\mathbf{s}_{k-1}^{(i^{(j)})}), \mathbf{Q})$.
- Compute $w_k^{(j)} \infty \frac{N(\mathbf{z}_k - \mathbf{h}(\mathbf{s}_k^{(j)}), \mathbf{R})}{N(\mathbf{z}_k - \mathbf{h}(\underline{\mu}_k^{(i^{(j)})}), \mathbf{R})}$.

3.3. Posterior Cramér-Rao Lower Bound

Under certain regularity conditions, see [7], the mean square *filtering* estimation error for each component of the state vector $\mathbf{s}_k$ is bounded from below by the posterior Cramér-Rao lower bound (CRLB) given by the diagonal entries of the inverse of the information matrix, $\mathbf{J}_k$, obtained from the joint density $p(\mathbf{s}_k, \mathbf{Z}_1^k)$. For a general nonlinear state-space model, $\mathbf{J}_k$ may be computed recursively for $k > 0$ using the algorithm described in [7]. The recursion in [7] involves however expectations that lack a closed-form analytical expression for the state-space model described by equations (1) and (5). We proceed then as in [2, 9] and replace those expectations with their Monte Carlo estimates obtained from simulated state trajectories. Further details are omitted here for lack of space.

4. SIMULATION RESULTS

We simulated the state model in (1) with parameters $g = 9.8\,m/s^2$, $\beta = 40000 kg.m^{-1}.s^{-2}$, $q = 5$, and $\Delta = 2\,s$. The initial state $\mathbf{s}_0$ was specified as a Gaussian random vector with mean $\mathbf{m}_0 = [232000\,m \;\; 2290\cos(190^o)\,m/s \;\; 88000\,m \;\; 2290\sin(190^o) m/s\,]$ and diagonal covariance matrix $\mathbf{\Sigma}_0$ with $\Sigma_0(1,1) = \Sigma_0(3,3) = 1000^2\,m^2$, and $\Sigma_0(2,2) = \Sigma_0(4,4) = 20^2 m^2.s^{-2}$. The measurements were simulated from the observation model (5) with parameters $\sigma_r = 100\,m$ and $\sigma_\epsilon = 0.017$ rad. The simulated target is tracked over 50 time steps using the improved SIR particle filter described in Section 3.1 with $N_p = 7000$ particles. That compares to a much higher number of particles (25000) previously reported in the literature [2] for a similar tracking problem with the same state model and a simpler, linear observation model. Figures 1(a) and (b) show the root-mean square error (RMSE) curves for the proposed filter's target position estimates, respectively in the x and y coordinates. The RMSE curves were estimated from 100 independent Monte Carlo runs. The SIR filter converged in all 100 simulations. For comparison purposes, we also plot in Figures 1(a) and (b) the square root of the corresponding posterior CRLB estimated from the same simulated state trajectories using the procedure briefly outlined in Section 3.3. The plots show that the RMSE curves match closely the bound for this particular set of simulations. In the sequel, we increased σ_r from $100\,m$ to $150\,m$ and increased $\sigma_{\dot{x}_0} = \sigma_{\dot{y}_0}$ from $20\,m/s$ to $50\,m/s$. Figures 2(a) and (b) show the corresponding RMS position estimate errors, respectively in the x and y coordinates, this time for both the improved SIR particle filter described in Section 3.1, and the auxiliary particle filter described in Section 3.2. We conducted again

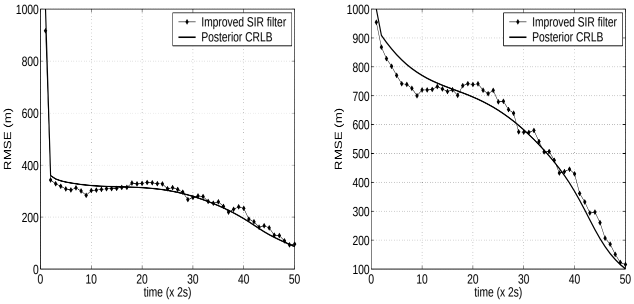

(a) (b)

Fig. 1. RMS position estimation error for the improved SIR filter with $\sigma_r = 100\,m$ and $\sigma_{\dot{x}_0} = \sigma_{\dot{y}_0} = 20\,m/s$; (a) x coordinate, (b) y coordinate.

100 independent Monte Carlo trials and used 7000 particles for both filters. As before, the RMSE curves are superimposed to the square root of the posterior CRLB for comparison purposes. Both trackers again converged in all 100 Monte Carlo runs. The improved SIR filter appears from the curves to outperform slightly the APF tracker. Further improvements in performance could probably be obtained by increasing the number of particles.

5. SUMMARY

We presented in this paper two improved particle filters for ballistic target tracking. The first filter uses an optimized importance function combined with residual resampling to minimize particle degeneracy, and also incorporates a Metropolis-Hastings move step to prevent particle impoverishment. The second proposed tracker is an auxiliary particle filter. Despite the use of significantly fewer particles than previously reported in the literature [2], simulation results show good performance for both filters when compared to the posterior CRLB for the mean square estimation error.

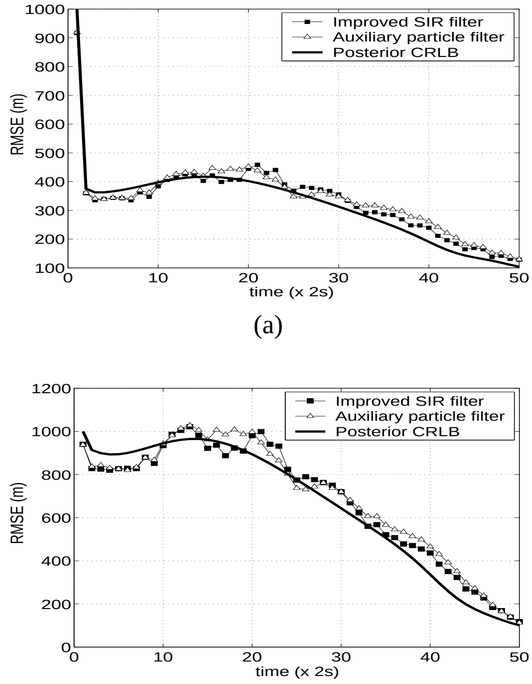

(a)

(b)

Fig. 2. RMS position estimation error for the improved SIR filter and the APF trackers with $\sigma_r = 150\,m$ and $\sigma_{\dot{x}_0} = \sigma_{\dot{y}_0} = 50\,m/s$; (a) x coordinate, (b) y coordinate.

6. REFERENCES

[1] M.S. Arulampalam, S. Maskell, N. Gordon, and T. Clapp, ”A tutorial on particle filters for on-line nonlinear/non-Gaussian Bayesian tracking,” *IEEE Transactions on Signal Processing*, vol. 50, n. 2, pp.174-188, February 2002.

[2] A. Farina, B. Ristic, and D. Benvenuti, “Tracking a ballistic target: comparison of several nonlinear filters,” *IEEE Transactions on Aerospace and Electronic Systems*, vol. 38, n. 3, pp.854-867, July 2002.

[3] N. J. Gordon, D. J. Salmond, and C. Ewing, “Bayesian state estimation for tracking and guidance using the bootstrap filter”, *Journal of Guidance, Control, and Dynamics*, vol.18, n.6, pp. 1434-1443, 1995.

[4] A. Doucet, “On sequential simulation-based methods for Bayesian filtering,” *Technical Report CUED/F-INFENG/TR 310*, Department of Engineering, University of Cambridge, UK, 1998.

[5] W. R. Gilks and C. Berzuini,“Following a moving target _ Monte Carlo inference for dynamic Bayesian models,” *J. R. Statist. Soc. B*, vol.63, pp. 127-146, 2001.

[6] M. K. Pitt and N. Shephard, “Filtering via simulation: Auxiliary particle filters,” *Journal of the American Statistical Association*, 94(446), pp. 590-599, 1999.

[7] P. Tichavský, C. H. Muravchik, and A. Nehorai,“Posterior Cramér-Rao Bounds for Discrete-Time Nonlinear Filtering,” *IEEE Transactions on Signal Processing*, vol.46, n.5, May 1998.

[8] J. S. Liu and R. Chen,“Sequential Monte Carlo methods for dynamic systems”, *Journal of the American Statistical Association*, 93, pp. 1032-1044, 1998.

[9] N. Bergman,“Posterior Cramér-Rao Bounds for Sequential Estimation,” chapter 15 in *Sequential Monte Carlo Methods in Practice*, Springer-Verlag, 2001.